Machine Learning Research Project

George Katsonis
American College of Thessaloniki
giorgos_katsonis@hotmail.com

Abstract

In this paper we introduce the basics of machine learning research in the field of image classification. First, we describe the relevant metrics that are used to evaluate model performance. Next, we present a brief overview of a number of important data-sets used for various image classification tasks. Finally, we present our model utilizing inception convolution modules in order to achieve 86% validation accuracy in CIFAR10, and going through the experimentation procedure, outlining possible future improvements.

1. Introduction

1.1. Metrics

The most commonly used metrics for the calculation of the performance of a machine learning algorithm are the average accuracy, the F1-score, the top-k error, and the confusion matrix. [9]

1.1.1 Average accuracy

The average accuracy is the number of correct predictions divided by the number of samples, it can be represented both as a fraction and as a percentile, though the latter is most common.

1.1.2 F1-score

The F1-score correlates the opposing metrics of precision and recall using the following formula:

$$F1 = 2 * \frac{1}{\frac{1}{precision} + \frac{1}{recall}}$$

Where:

- **Precision**: The number of true positive results divided by the predicted positive results.

$$Precision = \frac{TruePositives}{TruePositives + FalsePositives}$$

- **Recall**: The number of true positive results divided by all the results that should have been predicted as positive.

$$Precision = \frac{TruePositives}{TruePositives + FalseNegatives}$$

1.1.3 Confusion Matrix

The confusion matrix is not only useful as a metric for performance but also as a visualization. It is a table where one dimension is all the actual labels, and the other is all the predictions of the model. For every sample, an overlap between the label on x and the label on y is a correct prediction. When constructing a confusion matrix, a diagonal is created that contains the overlaps, and thus the correct predictions. This allows us to easily see not only how many mistakes our algorithm made, but also allows us to identify clusters of incorrect predictions that might be caused by relations inside our data [9].

1.1.4 Top-k error

The top-k error is a score that increases when the correct label is included in the top k predictions of the model based on probability. This means that for a top-1 error we will have an increase in score only if the top predicted class of the model is the correct one, while for a top-5 error it suffices for the correct label to be one of the top 5 predicted. Clearly, the larger the k, the easier it becomes to score high, and the more meaningless the score becomes.

1.2. Data-sets

In machine learning we see two types of research. The first is application-oriented research, where the paper will attempt to create a solution to a specific problem using machine learning. The second is generalized research, where the paper will push the state-of-the-art models in order to improve them, using standardized benchmarks to demonstrate the improvements. Application-oriented research often uses specialized data-sets relevant to the examined domain.

1.2.1 TrashNet

TrashNet [10] is a data-set used in waste classification. It contains 2527 images, taken from mobile devices, and categorized as: glass, paper, cardboard, plastic, metal, and trash. As most domain-specific data-sets, TrashNet is extremely small; however, a number of techniques, that will be discussed later, are used to increase the sample number. In this paper we will be focusing on generalized research data-sets. These data-sets usually contain a large number of samples and features, they are extremely well documented, and often have many variants, curated versions of the original data-set that caters to a specific learning requirement.

1.2.2 CIFAR

CIFAR [9] [14] [16] is perhaps the most well-known families of data-sets for image classification machine learning research. The most popular variants are the original CIFAR 100 and its predecessor CIFAR 10. CIFAR 10 [3] consists of 60000 32x32 color images divided equally in 10 classes. CIFAR 100 [4] while having the same number of samples and the same resolution as its predecessor, greatly increases the number of classes to 100. The 100 classes are equally divided to 20 super classes providing more general categorization. For example, the classes beaver, dolphin, otter, seal, and whale are part of the superclass aquatic mammals. Caltech 256, much like CIFAR 100, is a direct increase on Caltech 101's size and complexity. It contains 30,607 color images of different sizes, categorized unequally in 256 object classes and one additional clutter class, with each class containing at least 80 samples [1].

1.2.3 MNIST

MNIST is a very popular education and benchmarking data-set comprised of 70.000 images of handwritten digits. As a modified subset of NIST special databases 3 and 1, MNIST samples have been subjected to several normalization techniques in order to achieve a unified 29x29 grayscale resolution [6]. The most interesting aspect of this data-set is the amount of variants that share its name. The largest variant of MNIST is Fashion MNIST [5], a data-set of the same size and sample resolution as the original, meant to be a direct replacement of the original by its creator. The images in Fashion MNIST are of articles of clothing and the classes (remaining 9 as the digit classes of the original MNIST) are general clothing categories such as bag or trouser. MRDBI, or MNIST with Rotated Digits plus Background Images, dramatically increases the complexity of the original data-set in order to challenge the training models. Apart from the changes in the images indicated by the name, another factor of increased difficulty is the unusual split of the data to 12.000 training samples and 50.000 testing samples [9]. Other less known variants of MNIST include Chinese MNIST [2], which is comprised of 15.000 64x64 images of hand-drawn Chinese numbers, and sign language MNIST [16], a collection of 34627 24x24 grayscale samples representing hand signs categorized in 25 classes, one for each letter with no cases for 9=J and 25=Z since they require motion gesturing. The variants of MNIST are exceptionally different from the original; however, most generalized data-sets like CIFAR contain a very large number of variations created by slightly altering the images (i.e., flipping, mirroring, adding noise or distortion and even altering the colors). These techniques allow for exponentially increasing the number of samples in a data-set, or training models in specific ways [8] [18].

1.2.4 ImageNet

ImageNet [11] was the leading competition in image classification with machine learning. Despite the discontinuation of the competition, the benchmark data-sets used to facilitate it remain and are still widely used. Being perhaps the largest collection of labeled images, ImageNet contains over 15 million labeled high resolution pictures belonging to approximately 22,000 categories. Due to how vast the complete data-set is, there exist many subsets in order to make usage more accessible. One of those data-sets is the one used in the ImageNet Large-Scale Visual Recognition Challenge (ILSVRC). It contains approximately 1000 images in each category for a 1.2 million total training images, 50,000 validation images, and 150,000 testing images.

1.2.5 Benchmark data-sets

Due to the increasing rate of production for state-of-the-art models, there is a high demand for more streamlined and robust benchmarking solutions. Researchers [12] [13] [7] [17]create methodologies and data-sets that are meant to be used for the comparison of the performance for machine learning models for image classification. [7]

2. Proposed Model

2.1. Inception

The model we propose utilizes inception modules for convolutions instead of the baseline. An inception module consists of 5 layers, excluding the input layer. Those are:

- 1x1 convolution.
- 3x3 convolution.
- 5x5 convolution.
- 3x3 max pooling.
- Concatenation Layer.

The operations in the convolution and max pooling layer run independently and the resulting maps are concatenated to produce a single output. As shown in figure 2.1. [15]

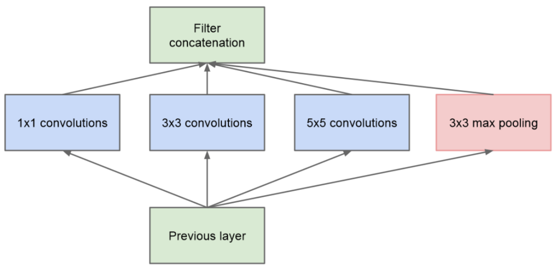

(a) Inception module, naïve version

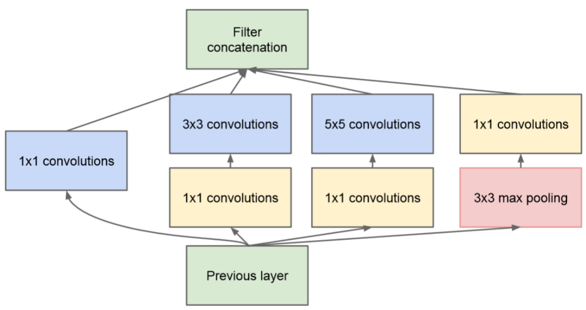

(b) Inception module with dimension reductions

Figure 1. Inception modules

2.2. Architecture - Data Flow

Layer	Feature Number
2D Convolution	864
ReLU	-
Batch normalization	128
2D Convolution	9,216
ReLU	-
Batch normalization	128
Inception 1	19,968
Dropout	-
Inception 2	24,064
Inception 3	82,944
Inception 4	329,728
Inception 5	1,314,816
Global average pooling 2D	-
Dropout	-
Dense	7690
Softmax	-
Total Features	1,789,546

Table 1. Model architecture

Configuration	Value
Padding Size	1
Window Size	3
Stride	1
Bias	None
Dropout Rate	0.4
L2 Regularization	True
Weight Decay	1e-4

Table 2. Module Configuration Parameters

2.3. Hyperparameters

Hyperparameter	Value
Epochs	50
Batch Size	128
Starting learning rate	0.05
Momentum	0.9
Cost Function	Categorical Cross-entropy
Optimizer	Stochastic Gradient Descent
Kernel initializer	Glorot uniform

Table 3. Model Hyperparameters

Epochs	Learning Rate
20	0.01
40	0.005

Table 4. Learning Rate Schedule

2.4. Data processing

The data has been standardized and some image augmentation has been implemented by randomly flipping the images. Random cropping was also attempted but never managed to reduce over-fitting, instead leading to overall worse performance for the model.

2.5. Model Performance

Model	Average Accuracy	F1-Score
Baseline	70%	0.7
Ours	86%	0.861

Table 5. Model Comparison

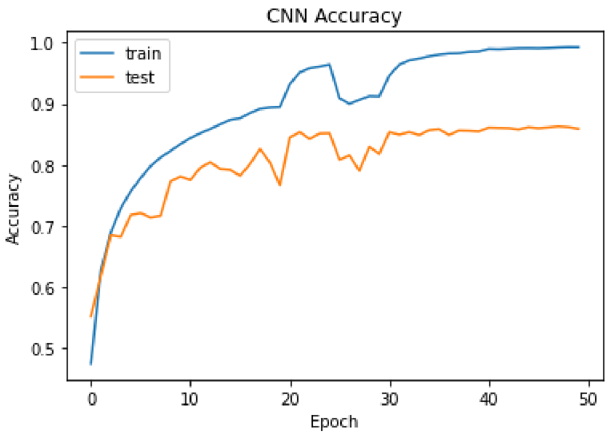

Figure 2. CNN Accuracy

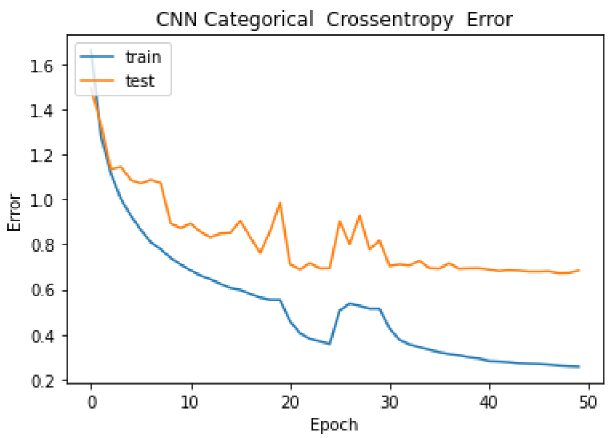

Figure 3. CNN Error

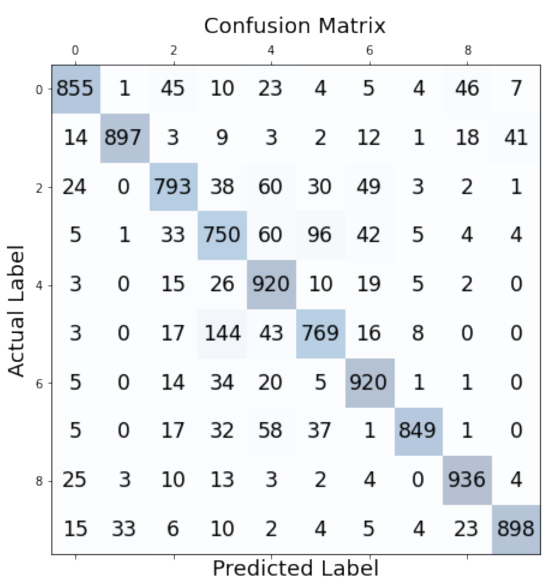

Figure 4. Confusion Matrix

3. Experiments

For the detailed account of the experimentation process please view the timeline. In this section we will outline some interesting observations, as well as an alternative model architecture.

3.1. Observations

- Standardization did nothing to improve over-fitting over regular normalization.
- Removing, moving, or adding more dropout layers drastically reduced performance no matter the other parameters.
- Random cropping image augmentation led to worse performance when used both in terms of training accuracy as well as over-fitting.
- Google collab will revoke your right to use a GPU if you forget terminating the run-time, leading to you not having graphs for the alternative model.
- Trying to avoid local minima by temporarily increasing the learning rate using the scheduler does work, by reducing the accuracy sharply before it returns to the plateau.
- 86% accuracy seems to be a hard limit for inception no matter the surrounding parameters.

3.2. Alternative model

Layer	Feature Number
2D Convolution	864
ReLU	-
Batch normalization	128
2D Convolution	9,216
ReLU	-
Batch normalization	128
Inception 1	19,968
Dropout	-
Inception 2	24,064
Inception 3	82,944
Inception 4	95,232
Inception 5	329,728
Basic Convolutional	442,880
Global average pooling 2D	-
Dropout	-
Dense	1290
Softmax	-
Total Features	1,006,442

Table 6. Alternative Model architecture

With this model we achieve 85.6% accuracy while reducing the number of features by 700,000 making the model significantly faster.

4. Conclusions

In this paper we presented an overview of the core metrics and datasets for image classification problems. We have presented two models that significantly improve on the baseline model's accuracy by using inception modules. Finally, we have recorded the observations made during our experiments. Points for future research would be the implementation of a Res-Net module, the experimentation with different cost and activation functions, different optimisers, as well as the implementation of adaptive learning rates that increase when the model plateaus.

5. References

References

[1] Caltech 256 Image Dataset. 2

[2] Chinese MNIST. 2

[3] CIFAR-10 and CIFAR-100 datasets. 2

[4] CIFAR-100 Python. 2

[5] Fashion MNIST. 2

[6] Papers with Code - MNIST Dataset. 2

[7] M. Caldeira, P. Martins, R. L. C. Costa, and P. Furtado. Image Classification Benchmark (ICB). *Expert Systems with Applications*, 142:112998, Mar. 2020. 2

[8] K. He, X. Zhang, S. Ren, and J. Sun. Deep Residual Learning for Image Recognition. *arXiv:1512.03385 [cs]*, Dec. 2015. arXiv: 1512.03385 version: 1. 2

[9] H. Iba and N. Noman. *Deep Neural Evolution: Deep Learning with Evolutionary Computation*. Springer Nature, May 2020. Google-Books-ID: jjPnDwAAQBAJ. 1, 2

[10] N. Karthikeyan. Review of Deep Transfer Learning Models for Image Classification. *International Journal of Recent Contributions from Engineering, Science & IT (iJES)*, 10(01):17–28, Mar. 2022. Number: 01. 2

[11] A. Krizhevsky, I. Sutskever, and G. E. Hinton. ImageNet Classification with Deep Convolutional Neural Networks. In *Advances in Neural Information Processing Systems*, volume 25. Curran Associates, Inc., 2012. 2

[12] Z. Lin, J. Shi, D. Pathak, and D. Ramanan. The CLEAR Benchmark: Continual LEArning on Real-World Imagery. page 13, 2021. 2

[13] V. Lomonaco. CORe50, Apr. 2022. original-date: 2017-04-25T17:56:29Z. 2

[14] S. Sankar, A. Jain, R. Chellappa, and S.-N. Lim. Regularizing deep networks using efficient layerwise adversarial training. May 2017. 2

[15] C. Szegedy, W. Liu, Y. Jia, P. Sermanet, S. Reed, D. Anguelov, D. Erhan, V. Vanhoucke, and A. Rabinovich. Going Deeper with Convolutions. (arXiv:1409.4842), Sept. 2014. arXiv:1409.4842 [cs] type: article. 3

[16] F. Wang, M. Jiang, C. Qian, S. Yang, C. Li, H. Zhang, X. Wang, and X. Tang. Residual Attention Network for Image Classification. *arXiv:1704.06904 [cs]*, Apr. 2017. arXiv: 1704.06904. 2

[17] T. Yellamraju, J. Hepp, and M. Boutin. Benchmarks for Image Classification and Other High-dimensional Pattern Recognition Problems. *arXiv:1806.05272 [cs, stat]*, June 2018. arXiv: 1806.05272. 2

[18] M. D. Zeiler and R. Fergus. Visualizing and Understanding Convolutional Networks. *arXiv:1311.2901 [cs]*, Nov. 2013. arXiv: 1311.2901 version: 3. 2